Colloids and Surfaces A: Physicochem. Eng. Aspects 487 (2015) 92–103

Contents lists available at ScienceDirect

Colloids and Surfaces A: Physicochemical and Engineering Aspects

journal homepage: www.elsevier.com/locate/colsurfa

Foam free drainage and bubbles size for surfactant concentrations below the CMC

John S. Lioumbas, Evanthia Georgiou, Margaritis Kostoglou, Thodoris D. Karapantsios*

Division of Chemical Technology, Department of Chemistry, Aristotle University of Thessaloniki, University Box 116, 541 24 Thessaloniki, Greece

HIGHLIGHTS

- Role of bubble size on the free drainage of moderately stable foams.
- Incorporation of data into the modified L–L model yields surface shear viscosity values.

GRAPHICAL ABSTRACT

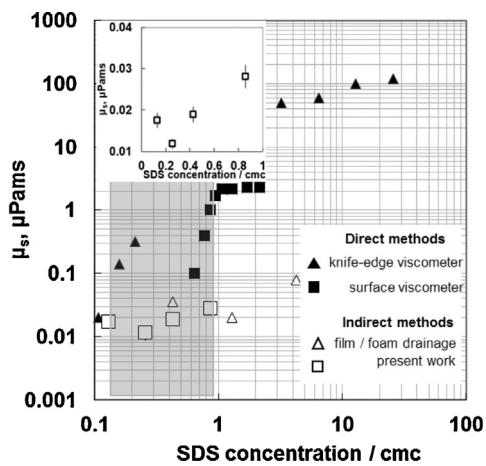

ARTICLE INFO

Article history:
Received 1 December 2014
Received in revised form
15 September 2015
Accepted 16 September 2015
Available online 25 September 2015

Keywords:
Free foam drainage
Bubble size
Moderately stable foam
Model
Coalescence
Coarsening
Below CMC

ABSTRACT

Foams produced with surfactant concentration below the Critical Micelle Concentration (CMC) are usually moderately stable due to high drainage rates and intense bubbles coarsening/coalescence. Aim of this work is to examine how such low surfactant concentration affects foam destabilization and elucidate the interplay between free drainage and bubble size variation. Foam destabilization experiments are conducted at varying SDS concentrations (below the CMC) where the evolution of liquid fraction and bubbles size is registered simultaneously. Instantaneous volume measurements of the drained liquid and the remaining foam yield the evolution of the global liquid fraction and drainage rate in the foam. Continuous electrical conductance measurements give the local liquid fraction and drainage rate in the foam. Microphotographs allow estimation of bubble size distribution and bubble population at regular time intervals. The present data show that the lifetime of moderately stable foams depend largely on surfactant concentration below the CMC but this effect does not scale linearly with surfactant concentration. Furthermore, measurements are fitted to semi-empirical expressions and are compared to a modified Leonard and Lemlich (L–L) drainage model that has been expanded to incorporate bubble size evolution. The latter is a rough approximation based on certain assumptions but it is a fair approach given the excessive difficulty of detailed numerical calculations. The comparison reveals the significant role of bubble size on the free drainage of moderately stable foams. Interestingly, incorporation of global liquid fraction data into the modified L–L model yields surface shear viscosity values in agreement with literature.

http://dx.doi.org/10.1016/j.colsurfa.2015.09.050
0927-7757/

1. Introduction

A foam comprises a mixture of liquid and bubbles, stabilized by surfactant, having an anisotropic distribution of liquid fraction and bubble size that both evolve dynamically [3,36]. Free foam drainage is a complex process since each of the following may take place simultaneously: gravitational liquid flow (liquid drains out of the foam chiefly through Plateau Borders (PB) and nodes), shear stresses imparted by the gas–liquid interfaces, capillarity induced liquid suction (opposing gravity especially at the foam bottom), bubbles size increase and bubble population decrease because of coalescence (merging of adjacent bubbles as result of rupture of the liquid films between them), and coarsening (enlargement of large bubbles by gas diffusion from smaller adjacent bubbles due to pressure differential between bubbles of unequal size-Ostwald ripening) [3].

The presence of surfactants in a foam can, in principle, influence both the gas–liquid interfacial properties (e.g., surface tension, surface dilatational viscosity, surface shear viscosity, surface elasticity) and the bulk liquid viscosity. Yet, for the bulk viscosity to be affected very large concentrations -well above the CMC- are required. Many preceding works (extended reviews on this topic can be found elsewhere e.g. [9,44] have shown that the type and concentration of surfactant modifies considerably the gas–liquid interfacial properties and, therefore, can change the flow type inside the foam's liquid network (i.e. PB, nodes and films) and can lead to significant alteration of drainage rates. However, most studies examine the above either in foam systems that maintain their initial bubbles size during drainage (i.e. surfactant concentrations well above the CMC and at high liquid fractions) or/and overlook the evolution of bubbles size, e.g., Cervantes-Martinez et al. [8], Boos et al. [3].

Several works have shown that bubble size evolution due to **coarsening** and free foam drainage are closely interrelated. Hilgenfeldt et al. [18], have shown that strong bubble coarsening leads to shorter drainage time (accelerated drainage) which is independent from the initial liquid content, ϵ_0. Both Magrabi et al. [25] and Vera and Durian [47] measured bubble size and liquid void fraction at various positions along the foam column during free drainage. Magrabi et al. [25] concluded that at their particular system, foam destabilization takes place at three stages: initially (<200s) drainage dominates over coarsening, later (200s–900s) drainage and coarsening occur concurrently and eventually (>900s) coarsening prevails over drainage. Vera and Durian [47] measured increased coarsening rates for drier foams and suggested that coarsening plays an unavoidable role in free drainage. Saint-Jalmes and Langevin [36] studied the coupling between drainage and coarsening of aqueous foams and showed that the type of flow inside the PBs depends on both bubbles size and gas–liquid interfacial properties. The above works do not take into account the effect of the type or/and surfactant concentration on the interaction between drainage and coarsening and, additionally, consider bubbles coalescence negligible.

It is known that for low surfactant concentrations, especially below the CMC, bubble **coalescence** may contribute significantly to bubble size variation during foam destabilization [10]. To the best of our knowledge, only Carrier and Colin [7], isolated bubble coalescence from coarsening by using a mixture of gases that has very low mass diffusivity in water. These authors examined the influence of various surfactants (i.e. SDBS and TTAB) at different concentrations on the interplay between coalescence and free drainage. They found that coalescence is dramatically enhanced below a critical liquid fraction which depends on the surfactant concentration and nature of the surfactant but does not depend on bubble size.

The only systematic work that we were able to identify on foam free drainage using surfactant **below** the CMC is that by Harvey et al. [17] These authors studied the effect of different types (i.e. Dowfroth-250, Dowfroth-400 and SDS) and different concentrations of surfactants (always below the CMC) on foam lifetime and on initial bubbles size. They showed that foam stability is controlled not only by the liquid drainage process, which is a function of surface shear viscosity, μ_s, but also by coalescence which is a function of other interfacial properties (e.g. surface dilatational viscosity of adsorbed layers). However, this study, being chiefly of technological orientation, did not investigate the effect of surfactant concentration on the evolution of bubble size and liquid fraction during foam drainage.

Scope of this work is to study the influence of surfactant concentration below the CMC on the interplay between bubbles size evolution (due to coarsening and coalescence) and free drainage. Surfactant concentrations below the CMC are used, because at these concentrations foams are only moderately stable. Novel data are presented concerning bubble size evolution and liquid fraction profiles both locally (electrical resistance measurements) and globally (volumetric measurements) for various surfactant concentrations. Additionally, it is examined if the present findings can be described by the well known drainage model of Leonard and Lemlich (1965, L–L model) [53] after incorporating the experimentally observed bubble size evolution to cope with coarsening and coalescence. In the following sections, the foam preparation procedure and a few essential physicochemical properties of the foam solution are presented first, being followed by an outline of the experimental setup and the employed measuring techniques. A section comes next with experimental results and discussion on the underlying phenomena.

2. Experimental setup and procedures

2.1. Foam preparation

Surfactant solutions are produced using deionized water and sodium dodecyl sulfate (SDS ≥ 98% purity; Fluka). Foams are produced employing four concentrations of SDS (300, 600, 1000 and 2000 ppm) which are below the reported CMC value at 30 °C (~2500 ppm). SDS is known for producing foams unstable with respect to coalescence [12]. A small amount of NaCl 4×10^{-3} M; (≥99% purity Merk) is added to deionized water to yield the ionic strength met in applications where foams are produced from fresh (mineral) water, typical for food and cosmetic applications. Prior to use, NaCl was heated to 550 °C to eliminate organic residuals. The use of NaCl in deionized water allows avoiding problems created by precipitation of calcium and magnesium salts in fresh water. In addition, this small concentration of NaCl does not affect interfacial properties whereas it permits reliable electrical measurements (see Section 2.3).

The surfactant is used as purchased without additional purification as it is not our intention to study the foaming performance of purified SDS but instead to compare the foaming performance of the same SDS at different concentrations below the CMC. Nevertheless, to check for the effect of impurities the equilibrium surface tension is measured at eight distinct concentrations over the examined range of concentrations (Wilhelmy plate method, TE2, LAUDA). The measured values at 30 °C are (±0.2 mN/m): 71.3 (0 ppm), 56.2 (300 ppm), 52.7 (450 ppm), 51.8 (600 ppm), 47.5 (800 ppm), 44.7 (1000 ppm), 41.9 (1300 ppm), 36 (1800 ppm) and 33.7 (2000 ppm). These values are in reasonable agreement-deviations from 0 to −4 mN/m with the only other mea-

* Corresponding author.
E-mail address: karapant@chem.auth.gr (T.D. Karapantsios).

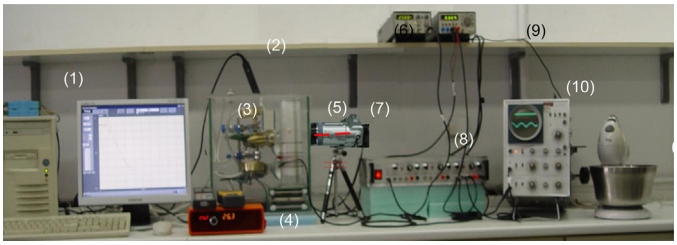

Fig. 1. Experimental layout: (1) Electrical data acquisition unit, (2) Digital Humidity recorder, (3) Temperature / humidity regulated chamber, (4) Thermal regulation unit, (5) Test cylinder for foam destabilization, (6) Function generator, (7) Digital camera for close-up photos (the camera for the instantaneous heights determination was positioned in front of the test cylinder), (8) Electrical signal analyzer, (9) Multimeter, (10) Oscilloscope, (11) Mixer for making foams. The two red solid lines on the test cylinder denote a pair of ring electrodes while the dashed red line shows the height where close-up photos are taken.

surements that were found in literature regarding (recrystallized) SDS with added 4×10^{-3} M NaCl [49]. Such small deviations might be attributed to the small temperature difference with that study (25 °C; [49]).

Foams are prepared by whipping air into 200 ml of the surfactant solution using a stand mixer (POWER PLUS, Izzy, 380 W) for 10 min. The turbulent mixing method (either by whipping or sparging) for producing foams has been applied by many researchers in the past (i.e. [21,36] Indrawati and Narsimhan [54]; [27,13,26,38]. This is because turbulent mixing can be met in a variety of technological applications such as processing of foods, detergents, cosmetics, pharmaceutics, firefighting foams etc. Moreover, according to literature [38,27] turbulent mixing is the most suitable method for rapidly producing large quantities of initially uniform and homogeneous foams. Part of the produced foam is immediately decanted to fill a cylindrical Plexiglas test container (70 mm id and 260 mm height) up to its top (initial volume of foam, $V_{F,0}$ = 987 ml) and is allowed to drain freely. The test container is put inside a special chamber where temperature and humidity are controlled (T = 30 ± 1 °C, relative humidity controlled by supersaturated NaCI solution at 75% ± 2%, measured by humidity sensor Honeywell HIH 4010 004). The experimental setup is presented in Fig. 1. Experiments are repeated five times.

2.2. Volumetric measurements

A still camera (SONY DSC-F717Cyber shot 5MP) is used to shot photographs of the whole foam column inside the test container at regular time intervals. These photographs are used to determine the instantaneous heights of the foam and of the drained liquid. From these values the instantaneous global volumetric liquid fraction, ϵ_{glob}, of the entire foam column are estimated using Eq. (1):

$$\epsilon_{glob} = \frac{V_{L,O} - V_L}{V_F} \quad (1)$$

where V_F is the instantaneous foam volume, V_L is the instantaneous drained liquid volume *and* $V_{L,0}$ is the initial liquid volume.

2.3. Local electrical measurements

Details of the electrical conductance technique can be found elsewhere [46]. The conductance gauge consists of two parallel stainless-steel rings (3 mm wide) running the internal circumference of the test container. The two rings are placed apart by 0.7 cm with the lowest ring mounted 5 cm from the bottom of the test container. The selection of the pair rings is such that their separation distance is large enough to average bubble size undulations yet small enough to preserve the local character of measurements [46].

Table 1
Initial (at the moment that the foam has been produced in the whipping vessel) foam and liquid fraction for various SDS concentrations created by whipping of $\boldsymbol{V_{L,0}}$ = 200 ml of liquid.

c_0	300	600	1000	2000
$V_{F,0}$, ml	1234.57	1369.86	1449.28	1680.67
$\epsilon_{0,}$ –	0.162	0.146	0.138	0.119

2.4. Close-up photos at the wall

High resolution close-up photographs of the foam are taken at regular time intervals (1 min) at a position located 15 cm from the bottom of the test container, using a still digital camera (CANON EOS 350D, 8MP) equipped with proper macro lens (CANON EF100 mm, f/2.8 Macro USM) and three extension rings (CANON, 13-21-31 mm) in order to attain the appropriate magnification. Average bubble diameters are determined from images (3.5mm × 3.5 mm) using custom made software based on a template matching technique which is capable of analyzing densely dispersed spherical bubbles in digital images [50]. The software identifies and analyzes only sharp focused bubbles in every image. For each surfactant concentration results are computed from five repetitive experiments (number of bubbles between ~500 and ~2000 for each time instant, reproducibility among repetitions ±5%). It has been recognized (Cheng and Lemlich [55]) that bubble distributions measured photographically at the wall may be different form the bubble size distribution in the bulk of the foam because the plane of view discriminates statistically against the inclusion of small bubbles. An algebraic treatment has been proposed to correct this statistical bias but errors such as bubble distortion and bubble segregation are tacitly ignored in most studies e.g. Magrabi et al. [24]. However, none of these errors affects the qualitative comparisons of this study [31].

3. Results and discussion

3.1. Evolution of drained liquid volume and foam volume

Table 1 presents initial foam volume produced by whipping 200 ml of the different surfactant solutions. As surfactant concentration increases *foamability* increases, too. This means that less initial liquid volume, $V_{L,0}$ is used to produce the same initial amount of foam, $V_{F,0}$and as a result the foam becomes dryer and more stable (i.e. initial global liquid fraction, ϵ_0, decreases). Fig. 2**a** presents the evolution of foam volume, V_F, and drained liquid volume, V_L, for different surfactant concentrations (i.e. 300, 600, 1000 and 2000 ppm); data points correspond to average measurements. The error bars at each data point stand for the standard deviation from five repetitions (average value ± 5% from repeatability runs). It is seen that at t = 0 there are small volumes of liquid and foam that have already been drained and collapsed, respectively. These initial volumes get smaller with increasing surfactant concentration – as foam stability increases – and are due to the inevitable foam drainage that takes place during transportation from the whipping vessel to the test container (time of transportation, $t_0 \sim 30$ s). As drainage proceeds, the volume of foam, $V_{F,}$decreases whereas the drained liquid, $V_{L,}$increases, both in a non-linear fashion. The V_F profiles decrease gradually when the surfactant concentration is higher than 300 ppm. However, for 300 ppm surfactant concentration, the V_F profile drops rapidly which indicates that the 300 ppm foam is unstable. All in all, the lifetime of the present moderately

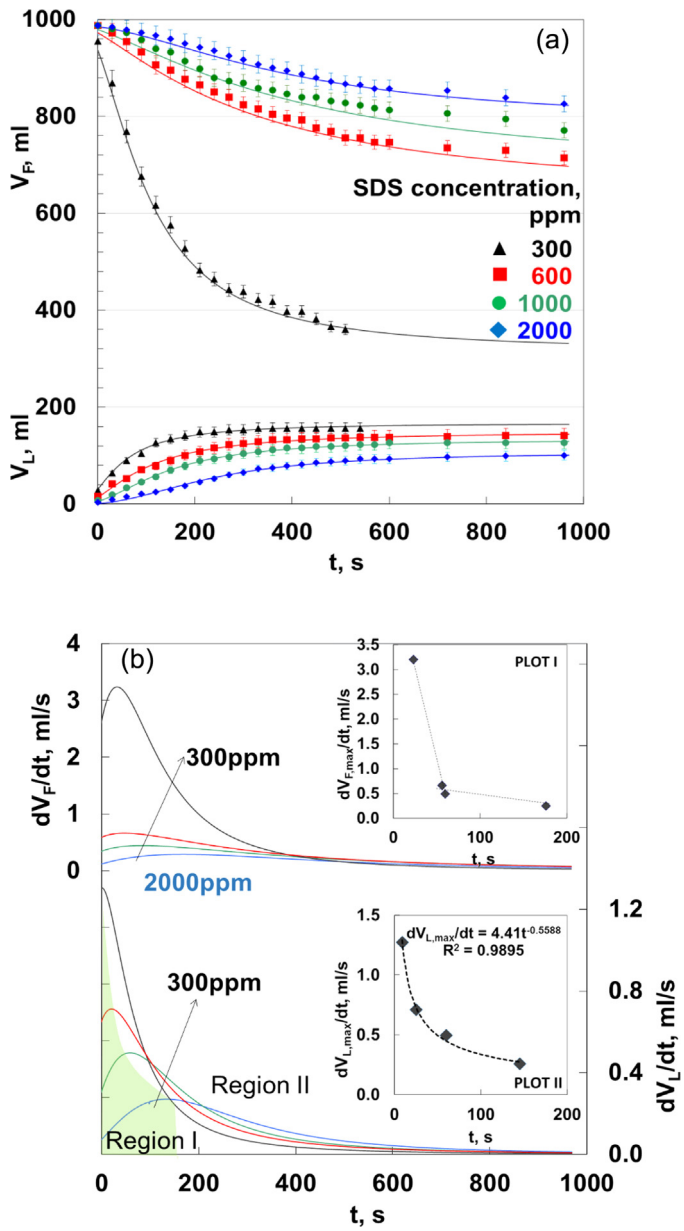

Fig. 2. Effect of SDS concentration on: a. evolution of foam volume, VF, and drained liquid, VL; b. Liquid drainage rate and foam volume decay rate profiles. Markers stand for raw data and lines for fitting equations and their derivative.

stable foams depend largely on surfactant concentration but this effect does not scale linearly with surfactant concentration.

The thin lines in Fig. 2**a** represent the V_L profiles fitted to an empirical expression, Eq. (2), that has been commonly used in literature to describe free foam drainage [6,51]:

$$A = \frac{V_F}{V_{L,O}} = \frac{1}{1 + \left(\frac{t+t_O}{T_F}\right)} \tag{2}$$

The V_F profiles are fitted to a similar expression:

$$B = \frac{V_F - V_{F,O}}{V_{F,\infty} - V_{F,O}} = \frac{1}{1 + \left(\frac{t+t_O}{T_F}\right) n_F} \tag{3}$$

$V_{F,\infty}$ is estimated from the fitting of Eq. (3) on the experimental V_F profiles and represents the theoretical foam volume at infinite time. T_L and T_F are the half-life for liquid drainage and foam decay whereas n_L and n_F are empirical parameters that describe the sigmoid character of the curves. A commercial software (TableCurve®) is used to determine the $V_{F,\infty}$, $T_{L,F}$ and $n_{L,F}$ values (Table 2). The produced sigmoid lines follow the data quite satisfactory ($R^2 \sim 0.996$–0.999). The sigmoid behaviour in V_L and V_F profiles has been reported in the past for various free drainage foam systems [4,19,39,25,47,28,48]. It must be stressed that the above equations are meaningful for time scales far from infinity, e.g., like those in the present study, for which $V_{F,\infty}$ take values much higher than zero.

Table 2
Fitting equation parameters for various SDS concentrations.

c_0	300	600	1000	2000
n_L, –	−1.59	−1.59	−1.85	−2.13
n_F, –	−1.77	−1.33	−1.40	−1.72
T_L, s	78.24	128	170.04	265.18
T_F, s	129.01	340	431	432
VF_∞, ml	315	628	678	784

Fig. 2**b** presents the derivatives of V_F (right axis, dV_F/dt) and V_L (left axis, dV_L/dt) for every tested surfactant concentration (i.e. 300, 600, 1000 and 2000 ppm). Data derivatives follow well the derivation of Eqs. (2) and (3). The sigmoid character of V_L and V_F results in a maximum (peak) value at the respective derivative profiles. The maximum, $(dV_L/dt)_{max}$, value separates the liquid drainage rate profiles in two distinct regions:

RegionI: At this region the drainage rate increases slowly until reaching $(dV_L/dt)_{max}$ at a specific time instant, t_{max}. Jacobi et al. [19] suggested that this initial increase should be attributed to the redistribution of the liquid content along the foam column. There are theories for a small induction period in the drainage process but they are associated to very stable foams with no liquid at the bottom initial state which is clearly not the case here [1]. The shape of the drainage rate curves may be seen as outcome of the combination of two phenomena. The first is the reduction of liquid content because of drainage and the second is the increase of bubble size because of coarsening and coalescence. Liquid flow resistance and, correspondingly, drainage rate depends on the cross-sectional area of PB. The reduction of liquid content with time leads to smaller PB cross sections (for constant number of PBs) and thus to smaller drainage rate. On the other hand, the reduction of the bubble number with time leads to a decrease of PB number and, consequently, to an increase of their cross-sectional area (for constant liquid content) resulting to higher drainage rates. The combination of the two phenomena – with different time evolution each – can lead to the observed sigmoid drainage curves. As surfactant concentration increases, the duration of *Region I* increases (t_{max} rises linearly with surfactant concentration) and the $(dV_L/dt)_{max}$ values decrease (i.e. following a power law function; $(dV_L/dt)_{max} \propto t_{max}^{-0.5588}$, embedded plot I in Fig. 2**b**). This implies that both competing phenomena are hindered (exhibit lower rates) as surfactant concentration increases. ***RegionII***: This region starts right after the inflection point. From this point on, the reduction of liquid content overwhelms the increase of bubble size and so drainage rate steadily decreases.

The dV_F/dt profiles appear to have a maximum point, $(dV_F/dt)_{max}$, too. The $(dV_F/dt)_{max}$ value for the lowest surfactant concentration (300 ppm SDS) is significantly higher (~5 times) compared to that at other concentrations. This indicates that the 300 ppm foam decays extremely faster than the other foams (embedded plot II in Fig. 2**b**).

3.2. Evolution of bubble size

Drainage rate and foam column stability are closely interrelated to foam bubble dynamics [25]. Fig. 3, presents bubble images, at a distance $H = 15$ cm from the test container bottom, at various

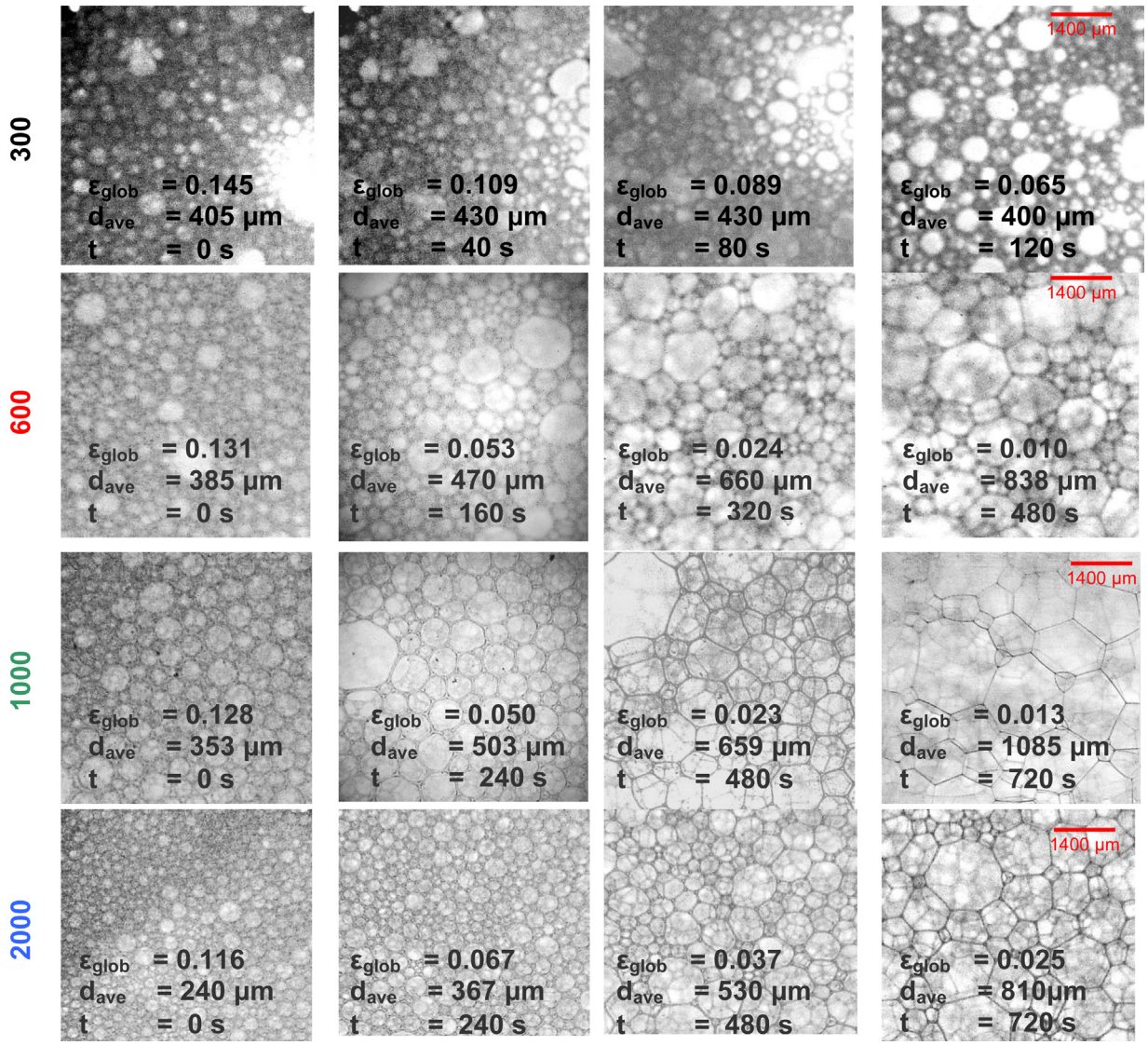

Fig. 3. Typical foam images during foam destabilization for various SDS concentrations.

time instants and various surfactant concentrations. The arithmetic mean bubble diameter, d_{ave}, calculated as suggested by Boos, et al [3]; Qian and Chen [56]; Stevenson et al. [57] and the global liquid fraction, ϵ_{glob}, are displayed inside the photos of Fig. 3. In principle, a Lagrangian observation of bubble size evolution is required. This is so because when drained liquid accumulates at the bottom of the foam it displaces the foam column upwards. In this case, bubbles observation should follow the foam motion. We performed tests by continuously removing the drained liquid from the foam bottom, and we have seen that the measured local liquid fraction is essentially the same with the case when no liquid is removed (Supplementary material). This indicates that the variation of foam features at the scale of foam displacement is insignificant, so an Eulerian observation (i.e. at a fixed position) of the bubble size distribution is permissible.

As SDS concentration increases, the foam becomes dryer (smaller ϵ_{glob}), the initial average bubble size, $d_{ave,0}$, decreases and as a result bubbles are more closely packed. For all examined SDS concentrations, initial bubbles are approximately spherical. As drainage proceeds, d_{ave} increases and bubbles shape deviates to polygonal. The case of the lowest examined surfactant concentration (300 ppm) is peculiar in the sense that the average bubble size remains approximately unchanged for the entire foam lifetime from production to collapse. Fig. 2**a**. (V_F data) indicates that for the 300 ppm foam (black markers) intense bubble collapse occurs at the top of the foam. This can cause high drainage rate at the top of the foam which can rewet the foam at lower heights and so bubbles size may stay unchanged.

Fig. 4 presents results from optical recordings. Fig. 4**a** presents the d_{ave}, evolution profiles during foam drainage for various surfactant concentrations. With the exception of the 300 ppm profile where only few data exist, all other profiles are successfully described by the same 2nd order polynomial equation that passes through $d_{ave,0}$ (dashed lines in Fig. 4**a**). This roughly indicates that for the examined surfactant concentrations bubble growth dynamics may be dictated by similar phenomena despite they start form different initial bubble diameter, $d_{ave,0}$ Furthermore, it is seen that $d_{ave,0}$ is strongly influenced by the SDS concentration ($d_{ave,0}$ decreases almost linearly with SDS concentration as shown in the inset plot). In the past, many studies have provided data concerning bubble evolution during foam drainage. Specifically, Magrabi et al. [24]; Gañán-Calvo et al. [16] and Feitosa and Durian [14], suggested that the average bubble size evolution increases at a decelerating rate according to the $r = t^{1/2}$ rule when coarsening phenomena

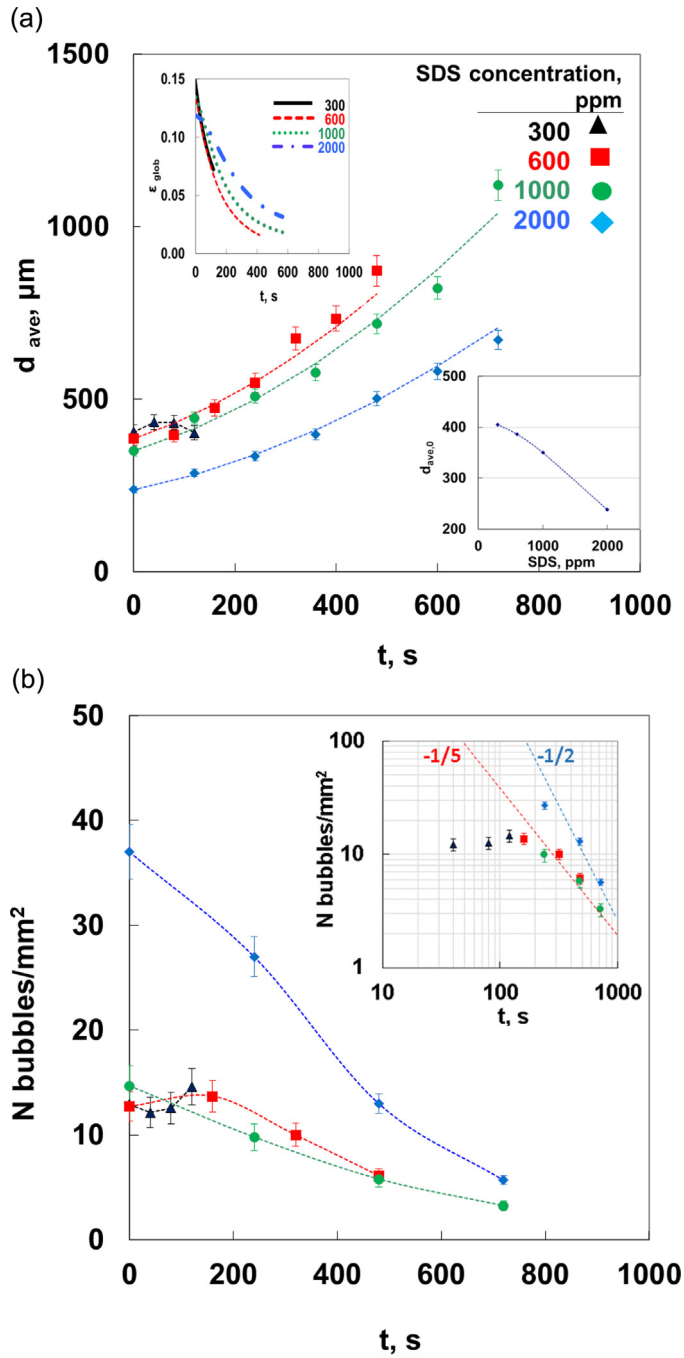

Fig. 4. Effect of SDS concentration on: a. arithmetic mean bubble size profiles (the embedded plot shows the dependence of the initial bubbles size on surfactant concentration and the liquid fraction evolution); the dashed lines represent the expression: $d_{ave} = d_{ave},0(2^{*}10{-}6^{*}t2 + 0.0013^{*}t + 1)$; ($R^2 = 0.993$) and b. Number of bubbles per area evolution during drainage (embedded plot in log–log coordinates). Bubbles are computed from still images running at a window frame of 3.5 × 3.5 mm.

are dominant. That trend is different than ours where bubble size increases at an accelerating rate. However, those other studies refer to very stable foams (far above the CMC) where coarsening alone, i.e., gas diffusion, governs bubble growth. In our moderately stable foams not only the liquid content changes considerably with time (liquid films and PBs get thinner) but also coalescence is occurring parallel to coarsening. Coalescence superimposes to coarsening and can yield an accelerating bubble growth with time as in Fig. 4**a**. More work is needed to elucidate this issue.

Bubbles population density (number per area) across the observation window is presented in Fig. 4**b** as a function of time for various surfactant concentrations. For surfactant concentrations up to 1000 ppm, the initial number (at $t = 0$ s) of bubbles, N_0, is small and rather independent from concentration. On the other hand, for 2000 ppm, N_0 is much higher. Moreover, the rate of bubble population change is alike for surfactant concentrations up to 1000 ppm but it is drastically higher for 2000 ppm. From a quick glance one might think that this contradicts the measurements in Fig. 2. However, this is not true. The 2000 ppm foam has many more bubbles than the other foams at lower SDS concentrations but of smaller size. In addition, given that the liquid content is comparable among all examined foams, the 2000 ppm foam has much thinner PBs. The existence of smaller bubbles with thinner PBs leads to higher curvature of intrabubble films and, therefore, increased capillary suction from the films to the PBs. The above is hampered by the effect of disjoining pressure and surface elasticity of the films which both rise with the concentration of surfactant. The net effect depends on the relative contribution of the above and in our case it is seen that bubble coarsening and coalescence are drastically stronger in the 2000 ppm foam. This is so although the drained liquid volume is small because as the surfactant concentration increases the rigidity of PB walls increases and so does also the hydrodynamic resistance to flow.

3.3. SDS concentration in the draining liquid

The SDS concentration in the liquid draining inside the Plateau Borders is expected to be smaller than the initial bulk liquid concentration due to adsorption to the bubbles surface. In order to examine if such depletion effects are important in our case, we calculated the surface coverage using the Gibbs equation. Specifically, the surfactant concentration in the draining liquid is computed from the surfactant mass balance:

$$V_{L,o}c_{s,O} + A_O T\left(c_{s,O}\right) + c_O V_{L,O} \tag{4}$$

where, $V_{L,0}$, $c_{s,0}$, A_0 and $\Gamma(c_{S,0})$ are the initial values (just right after foam formation) for, respectively, the volume of liquid inside the PBs, the surfactant concentration inside the PBs, the gas–liquid interfacial area and the surface coverage. The notation $V_L(t)$, $c_s(t)$, $A(t)$ is reserved for the time evolution of the corresponding variables. The SDS concentration in the initial bulk liquid (used to produce the foam) is denoted as c_0. A_0 can be calculated from Eq. (5), by employing the initial experimentally determined values for ϵ_{glob} and r_{ave} for each tested surfactant concentration:

$$A(t) = V_F(t)\frac{3\left(1 - \epsilon_{glob}(t)\right)}{r_{ave}(t)} \tag{5}$$

In fact, r_{ave} values vary along the height of the foam because coarsening and coalescence are usually faster at higher positions in the foam. However, as an approximation r_{ave} it is considered here constant along the foam. $\Gamma(c_{s,0})$ (presented Fig. 5**a**) is calculated by using the Gibbs equation (Eq. (6)) after replacing c_s with $c_{s,0}$ given that the static surface tension, γ, dependence on SDS concentration is experimentally measured:

$$T(C_s) = -\frac{c_s}{RT}\frac{d\gamma(s_s)}{dc_s}\left(1 + \frac{c_s}{c_s + c_{NaCl}}\right) \tag{6}$$

where c_{NaCl} is the salt concentration, R the ideal gas constant and T the system temperature [20]. We solve Eq. (4) numerically using Eqs. (5) and (6) to determine $c_{s,0,}$. Fig. 5**b** presents the c_s/c_0 dependence for the examined c_0 cases. Fig. 5**b** shows that immediately after foam formation ($t = 0$ s) the surfactant concentration inside the PBs is appreciably lower than c_0.

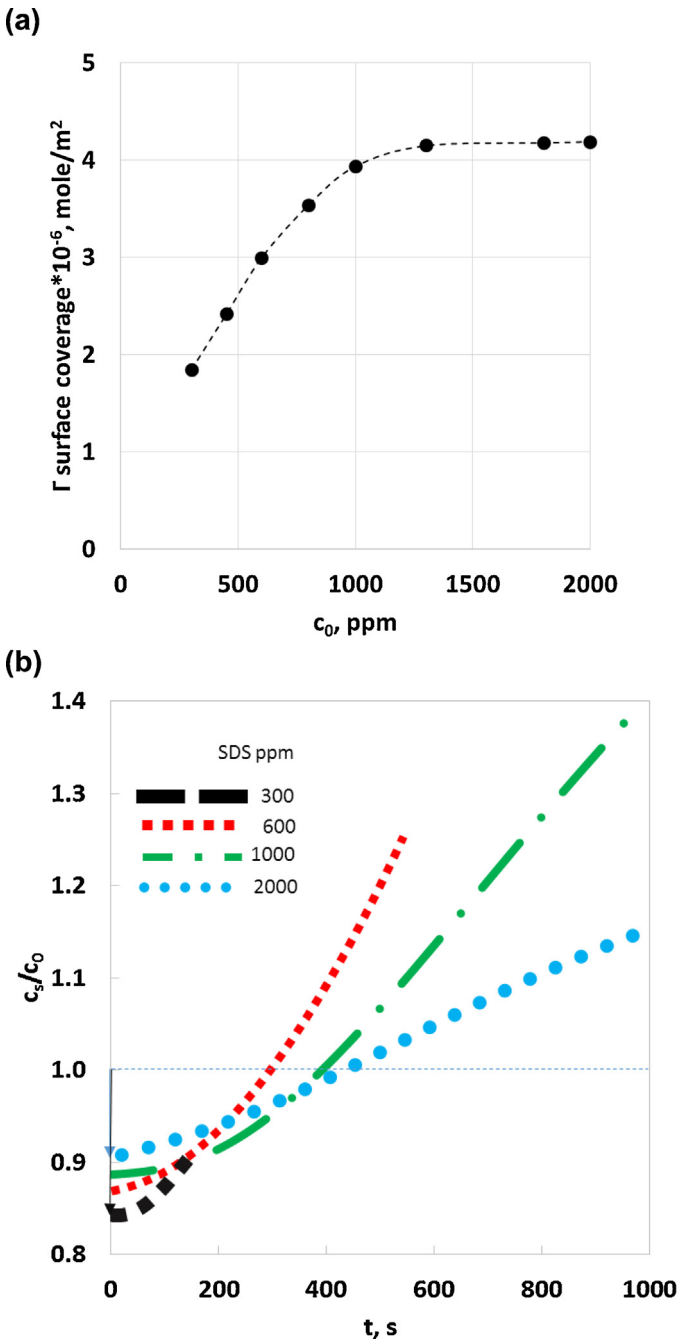

Fig. 5. (a) Surface coverage dependence on SDS concentration; (b) actual SDS concentration inside the foam liquid normalized over the initial SDS concentration during foam drainage.

The dynamic behaviour of c_s during drainage, can be found by solving the transient surfactant mass balance:

$$\frac{d}{dt}\left[V_L(t)+A(t)T(c_s(t))\right]=c_s(t)\frac{dV_L(t)}{dt} \tag{7}$$

Eq. (7) after differentiation yields:

$$\frac{dc_s(t)}{dt}=-T(c_s)\frac{dA(t)/dt}{V_L(T)+A(t)dT(c_s)/dc_s} \tag{8}$$

Eq. (8) is solved numerically using the initial conditions obtained by Eq (4). The time evolution of c_s is displayed in Fig. 5**b** for the various tested c_0 values. It is apparent that as drainage evolves and the bubble size increases, the surfactant concentration of the liquid draining to the PBs increases, too, and at some instant it becomes higher than c_0. The average value of c_s/c_0 over the entire examined drainage time is approximately (±3%) equal to 1. This indicates that the **average** c_s values are not expected to be significantly different than c_0 during the drainage process so the value c_0 can be considered as the independent variable for presenting our results.

3.4. Liquid fraction and foam uniformity

The upper half of the four plots in Fig. 6 (each one corresponds to a different surfactant concentration, i.e. 300, 600, 1000 and 2000 ppm) presents the profiles of the global (data points and thin fitting line) and the local liquid fraction, ϵ, (thick line) normalized with respect to the initial liquid fraction, ϵ_0. While instantaneous global liquid fraction, ϵ_{glob}, is calculated directly from the V_L over V_F ratio (Eq. (1)), the local liquid fraction, ϵ_{loc}, is computed from electrical measurements using a procedure proposed by Karapantsios and Papara [46] using the semi-empirical relation of Feitosa et al. [15]. At $t=0$ s, the $\epsilon_{glob}/\epsilon_0$ and $\epsilon_{loc}/\epsilon_0$ values are alike (for each surfactant concentration), which indicates a uniform initial liquid distribution along the foam column. These initial values are closer to unity as SDS concentration increases due to the smaller volume of drained liquid lost during foam transportation and decanting to the test container. As drainage proceeds the $\epsilon_{loc}/\epsilon_0$ values are higher than the $\epsilon_{glob}/\epsilon_0$ values because the foam is wetter near the bottom of the foam column where electrical measurements are taken [36]. However, during the last stages of drainage where the foam gets very dry $\epsilon_{loc}/\epsilon_0$ values approach $\epsilon_{glob}/\epsilon_0$ values. The exception observed for the 2000 ppm SDS concentration, indicates the existence of a significant volume of wet foam below the electrical measurement level, which contributes to higher ϵ_{glob} values. For free-draining foams it is known that if the drained liquid accumulates below the foam, the liquid can rise at the bottom layers of the foam and can yield volume fraction values even higher than the initial one [5,8]. This is more so for smaller bubbles, i.e. for 2000 ppm SDS, where capillary rise is prominent.

The lower half of the four plots in Fig. 6 presents the time derivatives of $\epsilon_{glob}/\epsilon_0$ and $\epsilon_{loc}/\epsilon_0$ profiles. The first peak on the $d\epsilon_{loc}/dt$ profiles at near zero time is due to the volume of liquid that has been drained in the whipping vessel before decanting to the test container. This reduces as surfactant concentration increases. The second peak observed in the above derivatives follows the same reasoning with the peak observed in the dV_L/dt profiles (Fig. 2**b**). With the exception of the 300 ppm foam, the $d(\epsilon_{loc}/\epsilon_0)$/dt profiles after the second peak appear qualitatively similar to the corresponding $d(\epsilon_{glob}/\epsilon_0)$/dt profiles. There is a time shift, t_r, between the two profiles (t_r is designated in Fig. 6**d**). This time shift corresponds to a delay for the propagation of liquid from the top to the bottom of the foam. Based on this notion, one may define an **effective propagation velocity** of the draining liquid, c, calculated from Eq. (9):

$$c=\left(h/t_{loc,max}\right) \tag{9}$$

where, h, is the distance between the initial level of the gas-foam interface (top of the foam) and the level of electrical measurements and $t_{loc,max}$ is the time necessary for the propagation of liquid to reach the electrical measurements level from the top of the foam ($t_{loc,max}$ is also designated in Fig. 6**d**). In free draining foams there is a continuous distribution of liquid velocities along the height of the foam and the effective propagation velocity, c, is just an engineering approximation of a characteristic draining velocity along the foam column. On this account, c must not be confused with the draining front velocity rigorously defined and clearly observed in forced drainage experiments (e.g. [40,32]).The estimated c values – shown inside the plots – decrease as surfactant concentration increases (with the exception at 300 ppm SDS where foam is extremely unstable). This indicates that the effective prop-

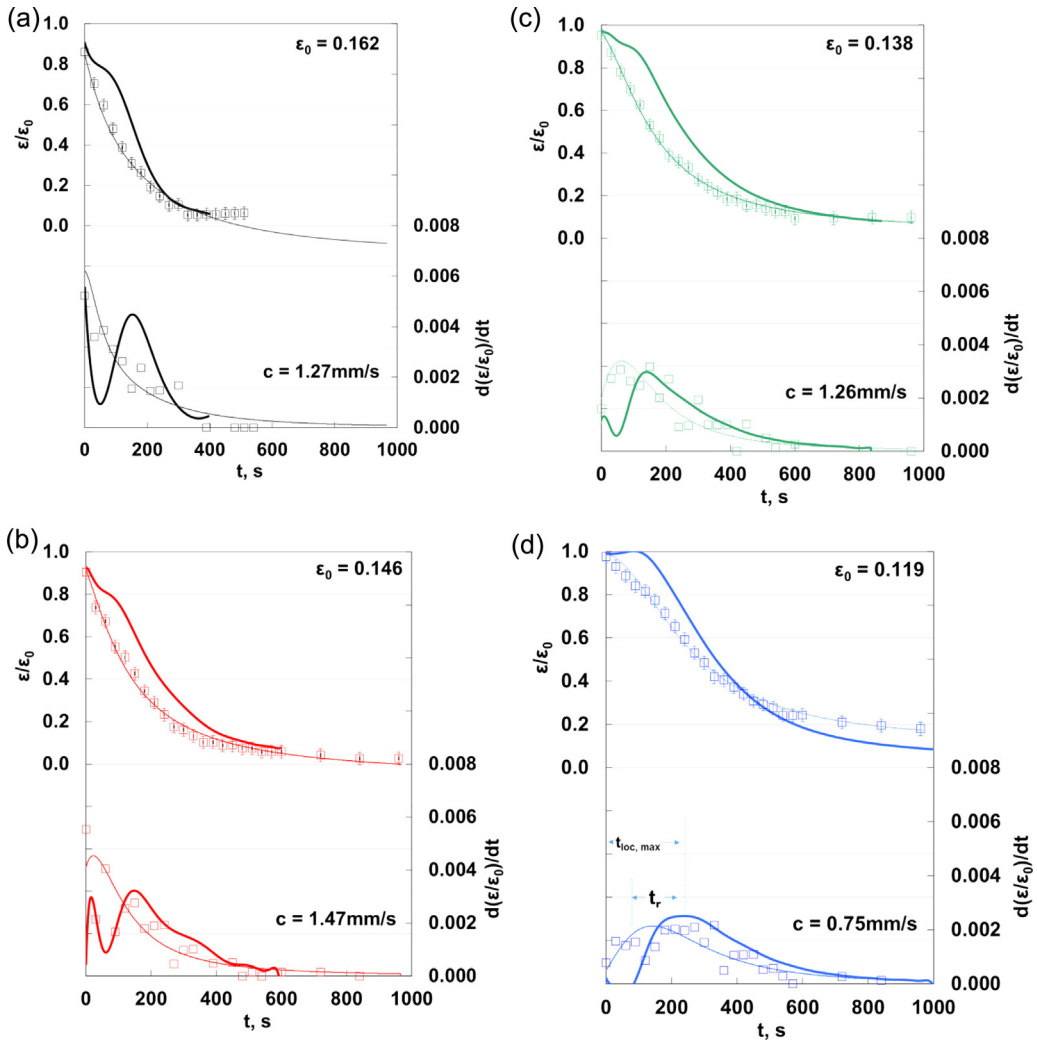

Fig. 6. Left axis: Liquid fraction profiles normalized with respect to the initial liquid fraction value, ϵ_0, obtained both locally (thick lines) and globally (markers); thin lines correspond to fitting curves. Right axis: Derivatives of the presented profiles. Effect of SDS concentration on the above profiles: a. 300 ppm, b. 600 ppm, c.1000 ppm and d. 2000 ppm.

agation velocity decelerates as surfactant concentration increases, in line with the more immobile PBs wall and the more dense bubble structure (i.e. smaller bubbles).

4. Comparison with model

Relation of measurable global drainage quantities to characteristics of a foam is not straightforward since free drainage is difficult to analyze. The situation is different from that of forced drainage where the front velocity is an easily measured variable directly related to foam characteristics [43]. In case of free drainage, there is a continuous spatio-temporal evolution of liquid fraction from the initial to the equilibrium state. This means that a complex spatially distributed foam model must be employed (incorporating many parameters for phenomena determining bubble size distribution e.g. [1], in order to compute the liquid fraction reduction in the foam. Direct modelling of the drainage process with simultaneous coalescence and coarsening is a very complex task not undertaken so far (in literature) in the context of comparison with experimental data. Our scope is indeed to undertake this difficult task but a careful step by step approach is needed. On this account, a first attempt to derive coalescence models based on experimental bubble size distributions has been made in Kostoglou et al. [23].

Here, we seek an alternative simple approach to allow a direct relation between free-draining foam characteristics and global liquid reduction rate. For this, we modified the well-known Leonard and Lemlich [53] model that describes the average drainage velocity at a cross-section of a foam with constant bubble size (no coarsening or coalescence). The modifications are based on three assumptions:

The first assumption is about using global quantities of liquid fraction and bubble size instead of local quantities at a cross-section of the foam, as is originally meant in the L–L model. This is of highly approximate nature (and the assessment of approximation requires further study) because as explained above there are complex spatial dynamics in the foam.

The second assumption is about ignoring capillarity effects when applying the L–L model to estimate global liquid reduction rates. Foam dynamics and the subsequent equilibrium is result of three opposing forces: gravity, on one hand, and capillarity plus shear stresses at the gas–liquid interfaces, on the other. Far from equilibrium, gravity and shear stresses are more important than capillarity so as a first approximation capillarity can be ignored in the model. The global liquid drainage rate is equal to the velocity through the Plateau borders at the bottom of the foam. Nevertheless, since the local liquid fraction is not-known at the bottom of the foam and, in addition, the capillarity has always a finite con-

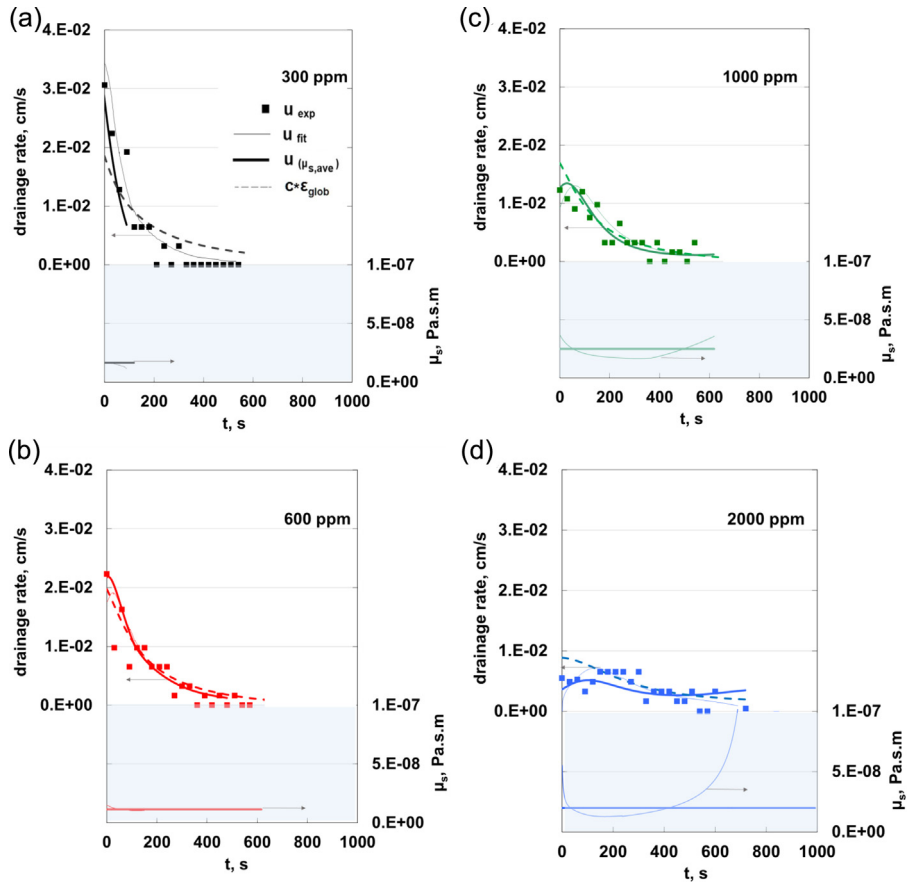

Fig. 7. Effect of SDS concentration on the drainage rate and shear viscosity profiles: a. 300 ppm, b. 600 ppm, c.1000 ppm and d. 2000 ppm. Left axis: Drainage rate: markers correspond to experimental drainage rate calculated from raw V_L data, thin lines are calculated from the V_L profile derivative, thick lines are calculated from the L–L model using average μ_s values, dashed lines are the product of the global liquid fraction profiles and the effective propagation velocity (superficial effective propagation velocity). Right axis: Average μ_s values (thick line), μs profiles derived from the L–L model (thin line).

tribution, at this point we make a compromise to cancel the effect of capillarity and so consider the global (average) liquid fraction in the corresponding velocity equation.

The third assumption is about considering coarsening and coalescence to be adequately described by incorporating in the L–L model the experimentally measured bubble size evolution. This ignores other than topological effects of coarsening and coalescence on drainage. The modified L–L model takes into account only one interfacial property, the surface shear viscosity, μ_s. The effect of other interfacial properties such as dilatational viscosity and dilatational elastic modulus, are included in the evolution of bubble size. It is well known (e.g., [42,34,17] that surface shear viscosity, controls the rigidity of PB walls and consequently the slip condition at the walls. In particular, **large** μ_s values correspond to **rigid** PB walls, maximum hydrodynamic resistance at the PBs and Poiseuille-like flow. On the contrary, **small** μ_s values correspond to **mobile** walls, maximum momentum losses at the nodes and plug-like flow [11,40,37]. Magrabi et al. [24], also extended the L–L model but used it in a different fashion, i.e., to predict bubble size distribution functions during bubbles coarsening by incorporating a change in liquid fraction.

Admittedly, the proposed use of the L–L model is a rough approximation valid only under certain assumptions However, it is an analytical approach that is worth to examine because of the excessive difficulty to obtain detailed numerical calculations.

The L–L model has been employed by many researchers in the past (i.e. [30,41] and [43] to predict the average superficial velocity, u_{sup}, (drainage rate) of the liquid flow over a cross-section of a foam (Eq. (10)). The factor of 1/3 arises from assuming that all Plateau borders within the network are randomly oriented [41]. It incorporates three different physical parameters: **A.** bubble size, **B.** liquid fraction, and **C.** flow resistance inside the PBs (expressed by the Boussinesq number, Bo, which includes the surface shear viscosity μ_s):

$$u_{sup} = \underbrace{\frac{(0.402r)^2\rho g}{3\mu}}_{\text{A(bubblesize).}} \underbrace{\epsilon}_{\text{B(liquidfraction)}} \underbrace{\left(0.02 + \frac{0.0655Bo_0{}^{-0.5}}{0.209 + Bo_0{}^{0.628}}\right)}_{\text{C(flowresistanceinPBs}} \quad (10)$$

where g is the gravitational acceleration, μ and ρ are the bulk viscosity and density, respectively, Bo is defined as the ratio of the surface to the bulk viscous stress, that is:

$$\text{Bo} = \frac{\mu_s}{\mu r} \quad (11)$$

r is radius of the PB walls curvature which can be expressed as a function of the bubbles radius, r_b, [43]:

$$r = 1.28\epsilon^{0.46} r_b \quad (12)$$

The L–L model can be used for the estimation of μ_s values if ϵ, u_{sup} and r_b values are known. In the present study u_{sup} values are calculated from global volumetric measurements of ϵ since electrical measurements provide only a balanced drainage rate on the measurement level. Therefore, u_{sup}, ϵ and r_b are calculated from the data presented in Figs. 2 **b**, 4 and 5, respectively.

The upper half of the four plots (left axis) in Fig. 7 presents the evolution of the drainage rate, for various surfactant concentrations. Specifically, data points stand for experimental drainage

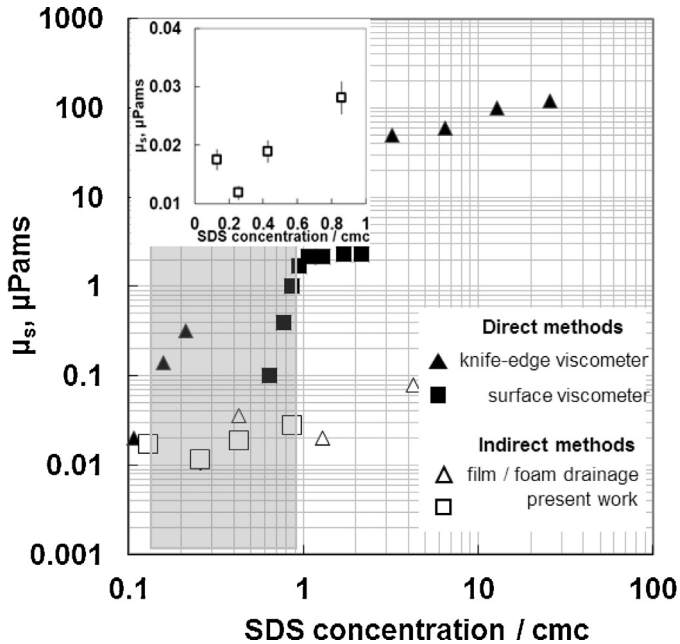

Figure 8. Measured values of surface shear viscosities μs as function of normalized SDS concentration over the SDS cmc. Closed markers correspond to direct measurements triangle: (group of higher values): Patist et al. [33], (group of lower values): Harvey et al. [17]; square: Poskanzer and Goodrich [35]. Open markers correspond to indirect measurements (triangles (from lower to higher SDS concentrations): Koehler et al. [22]; Pitois et al. [34]; Saint-Jalmes et al. [40]; square: present work). The shaded region denotes the SDS concentrations explored in this study.

rate, u_{exp}, (calculated from the raw V_L data: $u_{exp} = (1/A)^* dV_L/dt$, A is the foam column cross section), the thin line stands for the smoothed experimental drainage rate calculated by differentiation of Eq. (2), u_{fit}, and, finally, the dashed line represents the product of the global liquid fraction profiles and the effective propagation velocity (superficial effective propagation velocity). The latter follows satisfactory the decaying, and more lengthy stages, of u_{exp} and u_{fit} profiles but misses their initial rise, as expected.

In order to estimate μ_s profiles, u_{fit} data are employed in Eq. (10). These μ_s profiles are plotted at the lower half of the four plots (right axis) in Fig. 7 (thin line). The average values of the μ_s profiles over the whole period of drainage, $\mu_{s,ave}$, are also shown in Fig. 7 (thck line). Since in most studies so far, μ_s values have been considered constant during the drainage process, $\mu_{s,ave}$ values are incorporated in Eq. (10) to yield a drainage rate profile, u($\mu_{s,ave}$), based on constant μ_s values (thick line in the upper half of plots in Fig. 7).

As shown in Fig. 7, the L–L model, $u_{sup}(\mu_{s,ave})$, using an $\mu_{s,ave}$ value, predicts fairly well the measured drainage rate which indicates that foam permeability is controlled by viscous resistance in the Plateau borders ('channel-dominated flow') [45]. However, for the foam having the highest SDS concentration (2000 ppm), the model over-predicts the drainage rate values at the last stages of drainage (*Region II*). The computed μ_s profiles show larger μ_s values than the average ones during the last stages of *Region II* in this particular foam. Pitois et al. [34] performed film drainage experiments using SDS and also determined μ_s values that increase as the liquid flow rate decreases. They attributed this behavior to an increase in surface rigidity due to the surfactant saturation at the gas–liquid interface which results to additional effects such as Gibbs elasticity or dilatational viscosity, that are increasing as the interface is subjected to increasing stresses.

Fig. 8 compares the μ_s values from literature with the $\mu_{s,ave}$ values of this study. The error bars at each data point stand for the standard deviation from five repetitions (±10%). The μ_s values in literature are separated in two categories based on the type of measuring method: **direct** (invasive) and **indirect** (non-invasive) method [42]. Every **direct** method (e.g. a wall knife-edge viscometer [33,17], deep-channel surface viscometer [35], ferromagnetic microbutton probes [52] relies on the deformation of the surface shape without appreciable change in the area of the surface (an ideal setup would involve a surface flow with no dilatational motion) [29]. Every **indirect** method incorporates the experimentally determined u, ϵ and r_b values into theoretical expressions that are mainly based on the L–L equation to determine the μ_s values. The indirectly determined μ_s values of this study are close to others determined also indirectly but for totally different foam systems. It is noted that all the estimated μ_s values in literature -regardless method- present a clear increase with surfactant concentration c_0. A recent survey by Mayer and Krechetnikov [29], who inspected the entire group of μ_s values available in literature for SDS, suggests that there is a concentration dependence of surface shear viscosity, with a monotonic increase in μ_s below the CMC. Our estimations, also shown in Figure 8, are in agreement with the expected positive correlation between μ_s and the surfactant concentration. However, the μ_s value for the 300 ppm is over-predicted and do not follow the monotonic increase. This may be due to the very intense coalescence phenomena that take place at this low surfactant concentration which may influence drainage rates by additional means than by just altering the bubble size. In that case the third assumption in the modified L–L model would not be valid. However, we choose to present this value in order to show that the proposed methodology may not be applied to very unstable foams.

The experimental configurations that have been used previously to indirectly measure μ_s values are based either on steady state microscale foam/film systems [22,34] or in large scale spatial-temporal homogeneous foam systems [40]. In the above systems, many complexities met in the present study (i.e. bubbles coarsening and coalescence, non-uniform liquid fraction) are technically excluded (i.e. forced drainage in large scale experiments or maintaining constant flow rates and PB geometry at micro-scale experiments). It must be reminded that the original L–L model describes the interstitial flow and drainage in a **stationary** or moving foam of non-growing bubbles for steady state conditions. However, the fact that the μ_s values of the present study are in agreement with literature values implies that the L–L model may be useful to predict the drainage rate also in moderately stable foam systems where bubble size varies with time.

5. Conclusions

In this study we examine the effect of varying surfactant concentrations below the CMC on the free drainage of moderately stable foams. In such systems high drainage rates are combined with intense bubbles coarsening and coalescence.

Larger surfactant concentrations result to dryer foams, with a more packed structure. Concerning the drainage process, the successful fitting of a sigmoid equation on the drainage data reveals a maximum value on the drainage rate profiles. This maximum value is the result of the combining effect between the bubbles size increase (due to bubbles coalescence), liquid fraction reduction and flow resistance inside the PBs (expressed by the shear viscosity values of the surfactant solution). As the surfactant concentration increases, the maximum value decreases and appears at larger times. This behavior indicates that more stable foams are formed as the foam gets dryer. Apart from it, our data present an accelerating bubble growth with time which is ascribed to coalescence superposition to coarsening.

Experimental evidence shows that coarsening and coalescence rates increase at high surfactant concentrations (2000 ppm) where

the foam is more stable. This appears strange at first glance, but one needs to consider that at such high surfactant concentrations not only the PB walls become more rigid and oppose drainage but also the curvature of interstitial films gets higher due to the much smaller bubbles size and this favors coarsening and coalescence. Apparently, the observed foam stability at high surfactant concentration is dictated by the slow flow in the PBs and not by coarsening and coalescence.

There is a time shift, t_r, between the global and local liquid fraction measurements which corresponds to a delay for the propagation of liquid from the top to the bottom of the foam. This allows an effective propagation velocity of the liquid to be defined as an engineering approximation of a characteristic draining velocity along the foam.

A modified Leonard and Lemlich [53] has been suggested to relate global measurements of liquid fraction with foam characteristics. Although the proposed L–L model is valid only under certain assumptions it is found to provide realistic approximations for the examined systems. If confirmed by further work, this model may be useful to field engineers and technologists who do not have access to tedious numerical calculations or even to scientists asking for a first indication of foam performance.

Acknowledgments

The present activity was under the umbrella of COST Actions MP1106 and CM1101 and the European Space Agency funded programs: FASES (Fundamental and Applied Studies of Emulsion Stability) and PASTA (PArticle STAbilised Emulsions and Foams).

Appendix A. Supplementary data

Supplementary data associated with this article can be found, in the online version, at http://dx.doi.org/10.1016/j.colsurfa.2015.09.050.

References

[1] A. Bhakta, E. Ruckenstein, Decay of standing foams: drainage, coalescence and collapse, Adv. Colloid Interface Sci. 70 (1997) 1–123.
[3] J. Boos, W. Drenckhan, C. Stubenrauch, Protocol for studying aqueous foams stabilized by surfactant mixtures, J. Surfactants Deterg. 16 (1) (2012) 1–12.
[4] I. Cantat, S. Cohen-Addad, F. Elias, F. Graner, R. Höhler, O. Pitois, F. Rouyer, A. Saint-Jalmes, Foams Struct. Dyn. (2013).
[5] E. Carey, C. Stubenrauch, Free drainage of aqueous foams stabilized by mixtures of a non-ionic (C12DMPO) and an ionic (C12TAB) surfactant, Colloids Surf. A Physicochemical Eng. Aspects 419 (2013) 7–14.
[6] D.J. Carp, G.B. Bartholomai, A.M.R. Pilosof, A kinetic model to describe liquid drainage from soy protein foams over an extensive protein concentration range, LWT-Food Sci. Technol. 30 (3) (1997) 253–258.
[7] V. Carrier, A. Colin, Coalescence in draining foams, Langmuir 19 (11) (2003) 4535–4538.
[8] A. Cervantes-Martínez, A. Saint-Jalmes, A. Maldonado, D. Langevin, Effect of cosurfactant on the free-drainage regime of aqueous foams, J. Colloid Interface Sci. 292 (2) (2005) 544–547.
[9] N.D. Denkov, S. Tcholakova, K. Golemanov, K.P. Ananthpadmanabhan, A. Lips, The role of surfactant type and bubble surface mobility in foam rheology, Soft Matter 5 (18) (2009) 3389–3408.
[10] H. Do, M. Brady, D.P. Telionis, P.P. Vlachos, R. Yoon, Numerical modeling and experiments of coarsening foam, Int. J. Miner. Process. 98 (1–2) (2011) 66–73.
[11] M. Durand, D. Langevin, Physicochemical approach to the theory of foam drainage, Eur. Phys. J. E 7 (1) (2002) 35–44.
[12] E. Mileva, P. Tchoukov, Surfactant nanostructures in foam films, in: T.F. Tardos (Ed.), Colloid Stability: The Role of Surface Forces I, Wiley, Weiheim, 2007.
[13] J. Emile, A. Salonen, B. Dollet, A. Saint-Jalmes, A systematic and quantitative study of the link between foam slipping and interfacial viscoelasticity, Langmuir 25 (23) (2009) 13412–13418.
[14] K. Feitosa, D.J. Durian, Gas and liquid transport in steady-state aqueous foam, Eur. Phys. J. E 26 (3) (2008) 309–316.
[15] K. Feitosa, S. Marze, A. Saint-Jalmes, D.J. Durian, Electrical conductivity of dispersions: from dry foams to dilute suspensions, J. Phys. Condens. Matter 17 (41) (2005) 6301–6305.
[16] A.M. Gañán-Calvo, J.M. Fernández, A.M. Oliver, M. Marquez, Coarsening of monodisperse wet microfoams, Appl. Phys. Lett. 84 (24) (2004) 4989–4991.
[17] P.A. Harvey, A.V. Nguyen, G.J. Jameson, G.M. Evans, Influence of sodium dodecyl sulphate and Dowfroth frothers on froth stability, Miner. Eng. 18 (3) (2005) 311–315.
[18] S. Hilgenfeldt, S.A. Koehler, H.A. Stone, Dynamics of coarsening foams: accelerated and self-limiting drainage, Phys. Rev. Lett. 86 (20) (2001) 4704–4707.
[19] W.M. Jacobi, K.E. Woodcock, C.S. Grove Jr, Theoretical investigation of foam drainage, Ind. Eng. Chem. 48 (1956) 2046–2051.
[20] P. Joos, Dynamic Surface Phenomena, VSP, BV, Utrecht, 1999.
[21] S. Jun, D.D. Pelot, A.L. Yarin, Foam consolidation and drainage, Langmuir 28 (12) (2012) 5323–5330.
[22] S.A. Koehler, S. Hilgenfeldt, E.R. Weeks, H.A. Stone, Drainage of single Plateau borders: Direct observation of rigid and mobile interfaces, Phys. Rev. E Stat. Nonlinear Soft Matter Phys. 66 (2002) 40601/1–40601/4.
[23] M. Kostoglou, J. Lioumbas, T. Karapantsios, A population balance treatment of bubble size evolution in free draining foams, Colloids Surfaces A: Physicochem. Eng. Aspects 473 (2015) 75–84.
[24] S.A. Magrabi, B.Z. Dlugogorski, G.J. Jameson, Bubble size distribution and coarsening of aqueous foams, Chem. Eng. Sci. 54 (1999) 4007–4022.
[25] S.A. Magrabi, B.Z. Dlugogorski, G.J. Jameson, Free drainage in aqueous foams: model and experimental study, AIChE J. 47 (2) (2001) 314–327.
[26] K. Malysa, K. Lunkenheimer, Foams under dynamic conditions, Curr. Opin. Colloid Interface Sci. 13 (3) (2008) 150–162.
[27] S.P.L. Marze, A. Saint-Jalmes, D. Langevin, Protein and surfactant foams: linear rheology and dilatancy effect, Colloids Surf. A Physicochemical Eng. Aspects 263 (1–3) (2005) 121–128, 1SPEC. ISS.
[28] G. Maurdev, A. Saint-Jalmes, D. Langevin, Bubble motion measurements during foam drainage and coarsening, J. Colloid Interface Sci. 300 (2) (2006) 735–743.
[29] H.C. Mayer, R. Krechetnikov, Landau–Levich flow visualization: revealing the flow topology responsible for the film thickening phenomena, Phys. Fluids 24 (5) (2012).
[30] A.V. Nguyen, Liquid drainage in single Plateau borders of foam, J. Colloid Interface Sci. 249 (1) (2002) 194–199.
[31] M. Papara, X. Zabulis, T.D. Karapantsios, Container effects on the free drainage of wet foams, Chem. Eng. Sci. 64 (7) (2009) 1404–1415.
[32] C. Park, S.W. Hermanowicz, A multi-point electrical resistance measurement system for characterization of foam drainage regime and stability, AIChE J. 60 (9) (2014) 3143–3150.
[33] A. Patist, T. Axelberd, D.O. Shah, Effect of long chain alcohols on micellar relaxation time and foaming properties of sodium dodecyl sulfate solutions, J. Colloid Interface Sci. 208 (1) (1998) 259–265.
[34] O. Pitois, C. Fritz, M. Vignes-Adler, Liquid drainage through aqueous foam: study of the flow on the bubble scale, J. Colloid Interface Sci. 282 (2) (2005) 458–465.
[35] A.M. Poskanzer, F.C. Goodrich, Surface viscosity of sodium dodecyl sulfate solutions with and without added dodecanol, J. Phys. Chem. 79 (20) (1975) 2122–2126.
[36] A. Saint-Jalmes, D. Langevin, Time evolution of aqueous foams: drainage and coarsening, J. Phys. Condens. Matter 14 (40) (2002) 9397–9412, SPEC.
[37] A. Saint-Jalmes, Physical chemistry in foam drainage and coarsening, Soft Matter 2 (10) (2006) 836–849.
[38] A. Saint-Jalmes, M.U. Vera, D.J. Durian, Uniform foam production by turbulent mixing: new results on free drainage vs. liquid content, Eur. Phys. J. B 12 (1) (1999) 67–73.
[39] A. Saint-Jalmes, M.U. Vera, D.J. Durian, Free drainage of aqueous foams: container shape effects on capillarity and vertical gradients, Europhys. Lett. 50 (5) (2000) 695–701.
[40] A. Saint-Jalmes, Y. Zhang, D. Langevin, Quantitative description of foam drainage: transitions with surface mobility, Eur. Phys. J. E 15 (1) (2004) 53–60.
[41] P. Stevenson, C. Stevanov, Effect of rheology and interfacial rigidity on liquid recovery from rising froth, Ind. Eng. Chem. Res. 43 (19) (2004) 6187–6194.
[42] P. Stevenson, Remarks on the shear viscosity of surfaces stabilised with soluble surfactants, J. Colloid Interface Sci. 290 (2) (2005) 603–606.
[43] P. Stevenson, Dimensional analysis of foam drainage, Chem. Eng. Sci. 61 (14) (2006) 4503–4510.
[44] P. Stevenson, Foam Engineering: Fundamentals and Applications, John Wiley & Sons, Ltd., New York, NY, 2012.
[45] H.A. Stone, S.A. Koehler, S. Hilgenfeldt Durand, M, Perspectives on foam drainage and the influence of interfacial rheology, J. Phys. Condens. Matter 15 (1) (2003) S283–S290.
[46] T.D. Karapantsios, M. Papara, On the design of electrical conductance probes for foam drainage applications. Assessment of ring electrodes performance and bubble size effects on measurements, Colloids Surf. A Physicochemical Eng. Aspects 323 (2008) 139–148.
[47] M.U. Vera, D.J. Durian, Enhanced drainage and coarsening in aqueous foams, Phys. Rev. Lett. 88 (8) (2002) 088304/1–088304/4.
[48] J.R. Wagner, P. Sceni, Study on sodium caseinate foam stability by multiple light scattering, Food Sci. Technol. Int. 13 (6) (2007) 461–468.
[49] L. Wang, Surface Forces in Foam Films, in: PhD Dissertation, Virginia Polytechnic Institute and State University, 2006.
[50] X. Zabulis, M. Papara, A. Chatziargyriou, T.D. Karapantsios, Detection of densely dispersed spherical bubbles in digital images based on a template matching technique Application to wet foams, Colloids Surf. A Physicochemical Eng. Aspects 309 (2007) 96–106.

[51] Y. Yan, C. Qu, N. Zhang, Z. Yang, L. Liu, A study on the kinetics of liquid drainage from colloidal gas aphrons (CGAs), Colloids Surfaces A Physicochemical Eng. Aspects 259 (1–3) (2005) 167–172.
[52] Z.A. Zell, A. Nowbahar, V. Mansard, L.G. Leal, S.S. Deshmukh, J.M. Mecca, C.J. Tucker, T.M. Squires, Surface shear inviscidity of soluble surfactants, Proc. Natl. Acad. Sci. U. S. A. 111 (10) (2014) 3677–3682.
[53] R.A. Leonard, R. Lemlich, AIChE J. 11 (18) (1965).
[54] L. Indrawati, G. Narsimhan, Characterization of protein stabilized foam formed in a continuous shear mixing apparatus, J. Food Eng. 88 (2008) 456–465.
[55] H.C. Cheng, R. Lemlich, Ind. Eng. Chem. Fund 22 (105) (1983).
[56] S. Qian, J. Chen, Experimental investigation of liquid foams by polarised light scattering technique via the Mueller matrix, Chem. Eng. Sci. 104 (2013) 189–200.
[57] P. Stevenson, C. Stevanov, G.J. Jameson, Liquid overflow from a column of rising aqueous froth, Minerals Eng. 16 (2003) 1045–1053.